

Constraining the boundary between the Sunda and Andaman subduction systems: Evidence from the 2002 M_w 7.3 Northern Sumatra earthquake and aftershock relocations of the 2004 and 2005 great earthquakes

Heather R. DeShon

Department of Geology and Geophysics, University of Wisconsin-Madison, Madison, Wisconsin, USA

E. Robert Engdahl

Department of Physics, University of Colorado, Boulder, Colorado, USA

Clifford H. Thurber and Michael Brudzinski¹

Department of Geology and Geophysics, University of Wisconsin-Madison, Madison, Wisconsin, USA

Received 28 July 2005; revised 14 October 2005; accepted 9 November 2005; published 22 December 2005.

[1] The 2004 M_w 9.0 Sumatra-Andaman earthquake initiated along the Andaman subduction zone, north of the last great Sumatra earthquake along the Sunda Trench in 1861. During the 2005 M_w 8.7 Banyak Islands earthquake, a portion of the 1861 rupture subsequently failed. The boundary between the 2004 and 2005 ruptures broadly coincides with local trench rotation and the southern edge of the Andaman microplate, which suggests structural control on fault segmentation. Aftershock relocations of the 2004 and 2005 earthquakes show little overlap, and the sharp boundary between the series locates near the 2002 M_w 7.3 Northern Sumatra earthquake. We posit that these features represent the southern extent of the stable Andaman microplate, ~ 50 – 100 km northwest of what was previously reported. Broadband analyses of the 2002 earthquake yield a bilateral rupture pattern that is used to model Coulomb stress changes near the 2004 hypocenter to assess stress interactions along adjacent fault segments. **Citation:** DeShon, H. R., E. R. Engdahl, C. H. Thurber, and M. Brudzinski (2005), Constraining the boundary between the Sunda and Andaman subduction systems: Evidence from the 2002 M_w 7.3 Northern Sumatra earthquake and aftershock relocations of the 2004 and 2005 great earthquakes, *Geophys. Res. Lett.*, *32*, L24307, doi:10.1029/2005GL024188.

1. Introduction

[2] The seismic and tsunami hazard posed by great subduction zone earthquakes in the Sumatra region has long been recognized [e.g., *Newcomb and McCann*, 1987; *Sieh and Natawidjaja*, 2000]. In addition to the devastating 2004 M_w 9.0–9.3 Sumatra-Andaman Islands and 2005 M_w 8.7 Banyak Islands earthquakes, great earthquakes occurred along the Sunda subduction zone in 1797, 1833, and 1861. Short recurrence intervals of large to great earthquakes are not unprecedented in the region,

and understanding the role of fault segmentation and stress interactions along the subduction thrust has important implications for assessing seismic potential within the Sunda Trench.

[3] Rupture during the 26 December 2004 Sumatra-Andaman Islands earthquake (Figure 1) extended 1200–1300 km along the Andaman Trench and generated the most deadly tsunami in the historic record [*Lay et al.*, 2005]. The region had not recently hosted earthquakes of comparable size [*Bilham et al.*, 2005]. The aftershock sequence spans from northern Sumatra through the Nicobar and Andaman Islands (Figure 1). On 28 March 2005, a second great earthquake initiated along the Sunda Trench under the Banyak Islands. Rupture extended along ~ 400 km, primarily within the inferred failure region of the 1861 M 8.5 great Sumatra earthquake [*Lay et al.*, 2005] (Figure 1).

[4] Differences in upper and lower plate structure along Sumatra have been correlated to regions of repeated failure during great earthquakes [*Newcomb and McCann*, 1987; *Sieh and Natawidjaja*, 2000]. Two important tectonic features interact near the boundary between the 2004 and 2005 events: the southern edge of the developing Andaman microplate and a change in trench geometry (Figure 1). Additionally, the area has recently experienced two large underthrusting earthquakes—the 20 June 1976 M_w 7.0 and the 2 November 2002 M_w 7.3 events (Table 1).

[5] Aftershocks of the 2004 and 2005 earthquakes were relocated using the Engdahl, van der Hilst and Buland (EHB) method [*Engdahl et al.*, 1998]. The EHB locations illuminate the boundary between the two great earthquakes, which coincides with the location of the last large regional earthquake in 2002 (Figure 1). Based on these data, we reassess the location of the southern extent of the Andaman microplate. The temporal and spatial coincidence of the 2002 and 2004 events raises the question, did the 2002 earthquake impart significant stress changes at the eventual 2004 hypocenter? Broadband P and SH waveform analysis and surface wave empirical Green's function deconvolution of the 2002 earthquake provide a detailed rupture model that is used to predict

¹Also at Department of Geology, Miami University, Oxford, Ohio, USA.

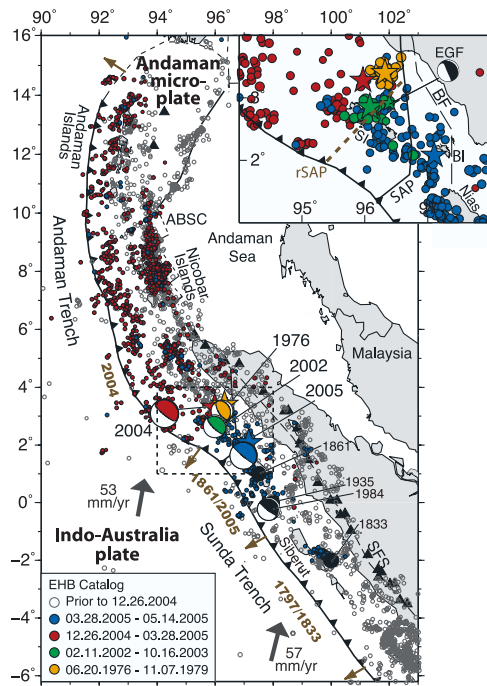


Figure 1. Tectonic and seismic setting of the Sunda and Andaman Trenches. EHB locations for the 1976 (orange), 2002 (green), 2004 (red), and 2005 (blue) mainshocks (stars) and aftershocks (circles) are shown. Brown arrows indicate the rupture boundaries of the 1797/1833, 1861/2005, and 2004 great earthquakes. Events discussed in the text are also shown (black circles or CMT solutions). Inset: Boundary between the 2004 and 2005 great earthquakes and the location of the EGF event. ABSC: Andaman backarc spreading center. BF: Batee Fault; rSAP: revised southern Andaman microplate boundary; SAP: southern Andaman microplate boundary; SFS: Sumatra fault system, SI: Simeulue. BI: Banyak Islands. Convergence directions are from *Sieh and Natawidjaja* [2000]. Plate boundaries are from *Bird* [2003].

Coulomb stress changes in the 2004 hypocentral region due to the 2002 earthquake.

2. Setting

[6] Indo-Australia and Eurasia plate convergence becomes increasingly oblique from south to north along Sumatra and the Andaman Islands. Offshore Sumatra, subduction occurs along the Sunda Trench, and motion along the megathrust is consistent with trench-normal underthrusting (Figure 1). The dextral strike-slip Sumatra Fault System (SFS) partitions the increasing obliquity to the north and transitions into the Andaman back-arc spreading center complex north of Sumatra [*McCaffrey et al.*, 2000]. This marks the eastern extent of the developing Andaman/Burma microplate (Figure 1). Formation of the southern boundary of the Andaman microplate has led to diffuse deformation in the forearc extending from the Batee Fault to $\sim 0.5^\circ\text{S}$ [*Sieh and Natawidjaja*, 2000]. North of this region, convergence along the Andaman subduction zone continues and

becomes nearly trench parallel along the northern Andaman Islands.

[7] The Sunda Trench has experienced multiple large and great earthquakes in the last ~ 200 years, with evidence for prior great earthquakes in 1797, 1833, and 1861 (Figure 1). For these events, rupture extent is based on seismic intensity and tsunami run-up reports, and hence epicenters are poorly constrained [*Newcomb and McCann*, 1987]. *Sieh and Natawidjaja* [2000], following *Newcomb and McCann* [1987], divided the Sunda Trench into segments based on seismic hazard potential and deformation features, including incoming plate structure and forearc basin development (Figure 1). Rupture during the 1797 and 1833 great earthquakes occurred along the southern segment of the Sunda Trench south of Siberut Island. Rupture during 1861 occurred along the central segment, the northern boundary of which is located between Simeulue and Banyak Islands. Between segments, megathrust rupture may occur during moderate magnitude earthquakes over shorter recurrence intervals (for example, the 1935 and 1984 events in Figure 1) [*Rivera et al.*, 2002].

[8] One of the most recent large earthquakes in northern Sumatra is the 1976 M_w 7.0 earthquake (Figure 1). Based on EHB locations and plate geometry, the megathrust should lie at ~ 30 – 40 km depth at its epicenter. The EHB 1976 mainshock depth is 15.3 km, and most of the aftershocks occur between 15–30 km depth. The Harvard Centroid Moment Tensor (CMT) solution depth is 19.1 km [*Ekström and Nettles*, 1997], and the centroid solution exhibits fault dips with a non-double couple component that is inconsistent with rupture along the shallow subduction thrust (Figure 1). The event likely ruptured a small forearc fault that accommodates oblique strain accumulation.

3. The 2002 M_w 7.3 Earthquake

3.1. Broadband Waveform Analyses

[9] We used body and surface wave modeling to better constrain the source mechanism and slip history of the 2002 underthrusting earthquake. Broadband body wave analysis followed the teleseismic inversion methods outlined in *Kikuchi and Kanamori* [1991] and *Kikuchi et al.* [1993]. We iteratively inverted P and SH body waves to solve for the combination of sub-events or rupture pattern that minimized data misfit. Particular attention was paid to trade-offs between focal mechanism, sub-event timing, velocity structure, and parameterization.

[10] P and SH misfit was minimized using two sub-events located at 28 km depth and the CMT solution (Figure 2). There was no evidence for complex rupture. P

Table 1. Source Parameters Taken From the EHB Catalog

Event	Date	Origin Time	Lat., °N	Lon., °E	Depth km	M_w
Northern Sumatra	06.20.76	20:53:12.7	3.44	96.25	15	7.0
Northern Sumatra	11.02.02	01:26:12.6	2.84	96.09	30	7.3
Northern Sumatra (EGF)	11.02.02	09:46:48.1	2.93	96.38	27	6.3
Sumatra-Andaman	12.26.04	00:58:53.4	3.29	95.97	30	9.0
Banyak Island	03.28.05	16:09:36.2	2.07	97.10	30	8.7

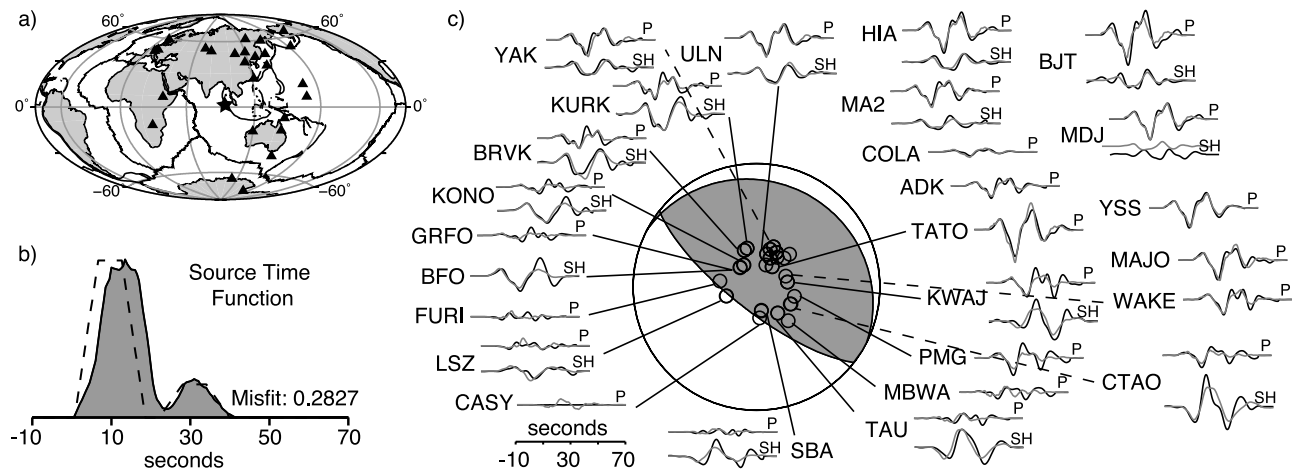


Figure 2. Body wave modeling solution. (a) Station distribution (triangles). Star: 2002 event. (b) Source time function of best-fit model (gray) and the initial simplified two subevent model (dotted line). (c) P and SH data bandpass filtered from 0.01 to 0.25 Hz (black) and modeled waveforms (gray) shown with the best-fit focal mechanism solution.

and SH data were inverted to solve for rupture along a fault plane parallel to the local strike of the Sunda Trench (297° strike, 16° dip). The best-fit solution fault plane (297° strike, 16° dip, 80° rake) had a residual error of 0.28 and total moment of $9.21E19$ N·m, M_w 7.24 (Figure 2), in good agreement with the CMT solution ($9.01E19$ N·m, M_w 7.2).

[11] We resolved rupture directivity for the 2002 earthquake using a surface wave empirical Green's functions (EGF) method described by *Ammon et al.* [1993]. For large earthquakes, moderate sized events with similar hypocentral and focal mechanism solutions can be deconvolved from the mainshock to remove path effects and isolate the relative source time function (RSTF) at individual stations. RSTF duration, t , is linearly related to mainshock source duration, t_o , directivity parameter, Γ , and rupture length, X , by

$$t = t_o - \Gamma X, \quad (1)$$

where $\Gamma \equiv \cos(\Phi - \Phi_o)/c$, Φ is the station azimuth relative to the source region, Φ_o the direction of unilateral rupture propagation, and c is the surface wave phase velocity. We solved for t_o , Φ_o , and X by finding the best linear fit over a range of rupture azimuths (see *Ammon et al.* [1993] for further details).

[12] We chose an M_w 6.3 aftershock located within 30 km of the 2002 mainshock as the EGF (Table 1; Figure 1). This event had a depth consistent with rupture on the subduction thrust and similar mechanism to the mainshock, though the EGF had a higher degree of right-lateral motion that causes additional noise in the RSTFs. Other earthquakes, including aftershocks of the 2004 and 2005 events, yielded poorer quality RSTFs.

[13] For both the EGF event and mainshock, teleseismic broadband data were rotated into vertical and tangential components, and the Love (L) and Rayleigh (R) waves were isolated using minimum and maximum group velocities (R: 5.0–2.2 km/sec; L: 5.5–2.2 km/sec). This resulted in 36 common stations with L and R waves (Figure 3a). Waveform quality following EGF-mainshock

water-level deconvolution was assessed based on signal-to-noise ratio and similarity of mainshock and EGF waveforms (Figure 3b).

[14] Most RSTFs exhibited a double peak and total duration similar to the source time function derived from P and SH data (Figure 3b). Source duration and directivity were solved for using RSTF onset and end time, average surface wave velocities (R: 3.85 km/sec; L: 4.38 km/sec), and station parameters. The best-fit solution yielded $X = 28 \pm 6$ km, $t_o = 39.6 \pm 0.7$ secs, and $\Phi_o = 290^\circ$ (Figure 3). Slip distribution was primarily bilateral, supporting the body

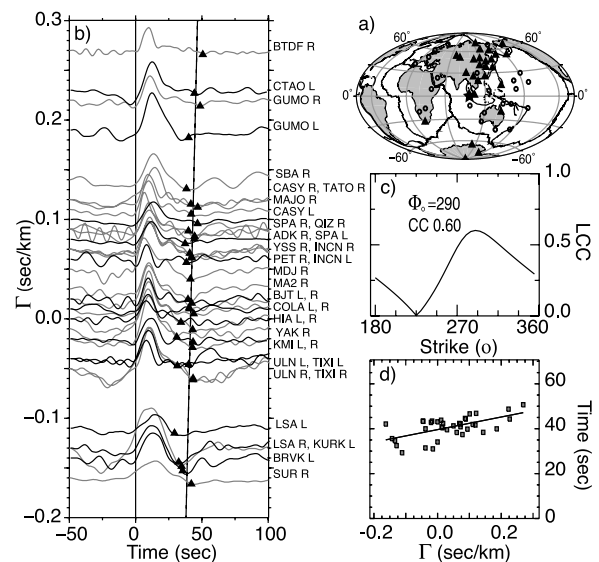


Figure 3. Surface wave EGF deconvolution. (a) Station distribution. Star: 2002 event. Triangles: Love and/or Rayleigh wave recordings. Open circles: Stations with poor data quality. (b) RSTFs for Love (black) and Rayleigh (gray) wave data. Triangles: RSTF duration. Vertical lines: onset and best fit. (c) The highest linear correlation coefficient was consistent with slip directed at 290° . (d) Least squares fit to duration versus directivity parameter data.

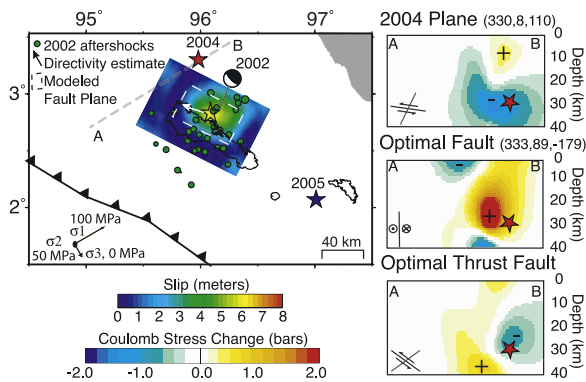


Figure 4. Coulomb stress analysis. (left) Slip distribution from broadband analysis, geometry of the 2002 fault plane, regional stress, and cross-section location. EHB mainshock locations (stars) and aftershock locations for the 2002 event (green circles) are shown. (right) Cross-sections of Coulomb stress changes shown with the EHB 2004 hypocenter (star) along faults oriented: (top) along the main failure plane of the 2004 earthquake, (middle) along optimally oriented faults, and (bottom) along optimally oriented thrust faults. Fault orientations are shown in bottom left corner in cross-section. All models were calculated with Coulomb 2.6 [Toda and Stein, 2002].

wave modeling results and consistent with the aftershock sequence (Figure 4).

3.2. Coulomb Stress Changes

[15] Studies of fault interaction and stress triggering have demonstrated that positive Coulomb stress changes correlate to increased aftershock activity and/or the hypocentral location of later large earthquakes [e.g., Toda and Stein, 2002]. For typical underthrusting earthquakes, the fault coincident with the along-strike edge of rupture will have a net Coulomb stress increase [Lin and Stein, 2004].

[16] We calculated Coulomb stress change due to the 2002 earthquake in the 2004 hypocentral region using a variable slip model consistent with the body wave rupture pattern and total moment (Figure 4). The CMT solution for the 2004 earthquake (330° strike, 8° dip, 110° rake) reflects the average failure orientation rather than the failure plane at initiation, here assumed to be at the EHB hypocenter. The Coulomb stress change for fault planes oriented with the CMT at 330° strike, 8° dip, and 110° rake was -1.0 to -0.6 bars within 10 km of the 2004 EHB hypocenter (Figure 4, top). However, the initial failure plane was potentially steeper than the average failure plane as the subducting plate dip increases with depth and distance from the trench and the CMT solution occurs well trenchward of the EHB epicenter (Figure 1).

[17] Failure could have alternately initiated on a plane optimally oriented for failure within the regional stress field. Most underthrusting focal mechanism solutions in the Sumatra region are consistent with trench-normal compression, or a regional maximum compressive stress (σ_1) striking at 60° (Figure 4). This orientation was taken as the regional σ_1 and used to calculate the orientation of optimally oriented faults in the 2004 hypocentral region. Optimally oriented failure planes for $\sigma_1=60^\circ$ are right-lateral strike-slip faults (330° strike, 89° dip, -179° rake) that

would have Coulomb stress changes due to the 2002 earthquake of $+0.8$ to $+1.2$ bars within 10 km of the 2004 hypocenter (Figure 4, middle). For optimally oriented thrust faults, Coulomb stress change was -0.6 to $+0.2$ bars (Figure 4, bottom).

[18] The 2004 hypocenter lies in a region sensitive to model parameterization and straddles the transition from positive to negative Coulomb stress change (Figure 4). We tested the sensitivity of the above results to the imposed regional stress field by computing the models with σ_1 strike varying from 10° (normal to the 2002 failure plane) through 70° . The tests yielded Coulomb stress changes of -1.0 to $+0.2$ bars in the 2004 hypocentral region for optimally oriented thrust faults, suggesting that regardless of σ_1 strike, the 2002 event did not significantly promote failure along thrust faults.

4. Summary

[19] In the region of the 2004 Sumatra-Andaman and 2005 Banyak Islands earthquakes, multiple tectonic features interact that may have influenced initiation and rupture during this great earthquake sequence. In 2004, the subduction thrust ruptured northward along the Andaman Trench and generated few aftershocks to the southeast [Lay et al., 2005]. In 2005, the megathrust failed to the southeast, and based on current plate boundary estimates, these aftershocks straddle the boundary between the Andaman and Sunda subduction zones (Figure 1, inset).

[20] Along northern Sumatra, trench strike varies from 330° in the 2004 and 2005 epicentral regions to 297° near the 2002 earthquake (Figure 1). Both the strike of the 2002 mainshock rupture plane and the long-axis of Simeulue reflect this local trench rotation, which suggests the well-developed geometry continues at depth. Trench rotation may be related to continuing development of the Andaman microplate and may affect stress interactions and strain transfer along strike by locally modifying the regional stress field. The Coulomb stress change analysis presented here was sensitive to the orientation of the regional stress field, and hence local perturbations to the regional estimate would affect the results. However, our results suggest that the 2002 event did not significantly promote thrust faulting in the 2004 hypocentral region.

[21] The development of the Andaman microplate boundary likely creates a diffuse deformation zone offshore Sumatra. We propose that the northern edge of this deformation zone is demarcated by the location of past large earthquakes such as the 2002 Northern Sumatra event and by the boundary between the 2004 and 2005 great earthquake aftershock series (Figure 1, rSAP). Our interpretation places the boundary ~ 50 – 100 km further northward than current estimates. The developing plate boundary likely served as a natural barrier to earthquake rupture to the southeast during the 2004 Sumatra-Andaman Islands earthquake and to the northwest during the subsequent 2005 Banyak Islands event.

[22] **Acknowledgments.** We thank S. Bilek for providing software and IRIS for providing waveforms. Comments by K. Sieh and an anonymous reviewer improved the manuscript. This work was supported by NSF grant EAR-0337495 to C. Thurber and E.R. Engdahl.

References

- Ammon, C., A. Velasco, and T. Lay (1993), Rapid estimation of rupture directivity: Application to the 1992 Landers (Ms=7.4) and Cape Mendocino (Ms=7.2) California earthquakes, *Geophys. Res. Lett.*, *20*, 97–100.
- Bilham, R., E. R. Engdahl, N. Feldl, and S. P. Satyabala (2005), Partial and complete rupture of the Indo-Andaman plate boundary 1847–2004, *Seismol. Res. Lett.*, *76*, 299–311.
- Bird, P. (2003), An updated digital model of plate boundaries, *Geochem. Geophys. Geosyst.*, *4*(3), 1027, doi:10.1029/2001GC000252.
- Ekström, G., and M. Nettles (1997), Calibration of the HGLP seismograph network and centroid-moment tensor analysis of significant earthquakes of 1976, *Phys. Earth Planet. Int.*, *101*, 219–243.
- Engdahl, E. R., R. van der Hilst, and R. P. Buland (1998), Global teleseismic earthquake relocation with improved travel times and procedures for depth determination, *Bull. Seismol. Soc. Am.*, *88*, 3295–3314.
- Kikuchi, M., and H. Kanamori (1991), Inversion of complex body waves 3, *Bull. Seismol. Soc. Am.*, *81*, 2335–2350.
- Kikuchi, M., H. Kanamori, and K. Satake (1993), Source complexity of the 1988 Armenian earthquake-evidence for a slow after-slip event, *J. Geophys. Res.*, *98*, 15,797–15,808.
- Lay, T., et al. (2005), The great Sumatra-Andaman earthquake of 26 December 2004, *Science*, *308*, 1127–1133.
- Lin, J., and R. S. Stein (2004), Stress triggering in thrust and subduction earthquakes and stress interaction between the southern San Andreas and nearby thrust and strike-slip faults, *J. Geophys. Res.*, *109*, B02303, doi:10.1029/2003JB002607.
- McCaffrey, R., P. C. Zwick, Y. Bock, L. Prawirodirdjo, J. F. Genrich, C. W. Stevens, S. S. O. Puntodewo, and C. Subarya (2000), Strain partitioning during oblique plate convergence in northern Sumatra: Geodetic and seismologic constraints and numerical modeling, *J. Geophys. Res.*, *105*, 28,363–28,376.
- Newcomb, K. R., and W. R. McCann (1987), Seismic history and seismotectonics of the Sunda Arc, *J. Geophys. Res.*, *92*, 421–439.
- Rivera, L., K. Sieh, D. Helmberger, and D. Natawidjaja (2002), A comparative study of the Sumatran subduction-zone earthquakes of 1935 and 1984, *Bull. Seismol. Soc. Am.*, *92*, 1721–1736.
- Sieh, K., and D. Natawidjaja (2000), Neotectonics of the Sumatran fault, Indonesia, *J. Geophys. Res.*, *105*, 28,295–28,326.
- Toda, S., and R. S. Stein (2002), Response of the San Andreas fault to the 1983 Coalinga-Nunez earthquakes: An application of interaction-based probabilities for Parkfield, *J. Geophys. Res.*, *107*(B6), 2126, doi:10.1029/2001JB000172.

M. Brudzinski, H. R. DeShon, and C. H. Thurber, Department of Geology and Geophysics, University of Wisconsin-Madison, Madison, WI 53706, USA. (hdeshon@geology.wisc.edu)

E. R. Engdahl, Department of Physics, University of Colorado, Boulder, CO 80309, USA.